Dielectric Characterization of Embedded Capacitance Films at Microwave Frequencies

J. Obrzut and R. Nozaki[1)]
NIST, Polymers Division
Gaithersburg, MD 20899

ABSTRACT
The dielectric permittivity and impedance characteristics were evaluated for high-dielectric constant polymer composite films that are being developed by the industry for Embedded Decoupling Capacitance applications. In order to extend the measurements to the microwave range, we developed a new testing methodology. The film specimen is treated as a distributed network consisting of a transmission line with the capacitance terminating a coaxial air-line. The theoretical model takes into consideration the wave propagation in the specimen section, thus eliminating limitations of the lumped element approximations. The implemented coaxial test fixture utilizes a simple 3 mm diameter disk test specimen. Using the new test technique, the dielectric permittivity of several EDC materials was evaluated at frequencies from 100 MHz to 10 GHz, and the impedance characteristics were determined directly in the time domain. The mechanism of dielectric relaxation in high dielectric constant films was studied using model polymer resins filled with ferroelectric ceramic powder. Based on these results, the desirable materials dielectric characteristics are discussed from the viewpoint of designing efficient embedded decoupling capacitance for high-speed circuits.

INTRODUCTION

Transient depressions of voltage driving devices (VDD or power to ground voltage), generated in the power lines of electronic circuits by fast processors and switching devices, limits their processing speed. De-coupling capacitors serve as a rapid source of charge to stabilize the VDD level and thus eliminate the associated electromagnetic interference noise (EMI). Current technologies utilize surface mounted discrete chip capacitors, which can effectively extinguish the power-bus noise at frequencies below 10 MHz. At higher frequencies, between 10 MHz and 100 MHz, only capacitors with the lowest connection inductance are able to source the charge. As the operating frequency increases above several hundred MHz all the discrete capacitors become ineffective and the VDD level can be stabilized solely by the inter-plane capacitance [1]. Thus, the closely spaced power-ground inter-plane arrangement can function as an embedded de-coupling capacitance (EDC). Throughout a multidisciplinary effort of the EDC Consortium, led by the National Center for Manufacturing Science (NCMS), it has been found that composites of polymer resins with ferroelectric ceramic can be extremely useful in constructing embedded de-coupling capacitance and power planes with low impedance over a broad frequency range, including the microwave [2]. In order to develop and successfully commercialize such materials, the industry needs a suitable broadband test method to measure the dielectric properties and to assess the impedance characteristic in planar, thin film configuration. However, the existing test procedures for thin films are based on lumped element approximations, which fail to produce meaningful results at microwave frequencies [3], especially in the case of high-dielectric constant films.

In this paper we describe a testing procedure that was developed to evaluate the impedance and dielectric permittivity of EDC films. The dielectric permittivity of several EDC materials that have been developed by the industry for de-coupling applications was accurately determined at frequencies of 100 MHz to 10 GHz. The methodology was also used to study mechanism of dielectric relaxation in model high dielectric constant polymer composites. Based on these results, the desirable materials dielectric characteristics are discussed from the viewpoint of designing efficient embedded decoupling capacitance that would secure the signal integrity and minimize the EMI noise in high-speed circuits.

THEORETICAL ANALYSIS

Input admittance of thin film capacitance with wave propagation terminating a transmission line

The experimental arrangement under consideration is shown in Figure 1. A dielectric circular film (or disk) sample of thickness d is placed at the end of a center conductor of known air-filed coaxial waveguide. The diameter of the sample f matches that of the center conductor. The sample is covered with a counter conductor directly extending from an outer conductor of the coaxial waveguide to form a circular parallel-plate capacitor. The primary propagation mode in the specimen section is associated with multiple reflections along the diameter of the film specimen [4]. Electrically, this structure is equivalent to a network in which the sample section can be viewed as a depressive transmission line inserted between two matched transmission lines. According to reference [5], the

[1)] Permanent address: Division of Physics, Graduate School of Science, Hokkaido University, Sapporo 0810, Japan

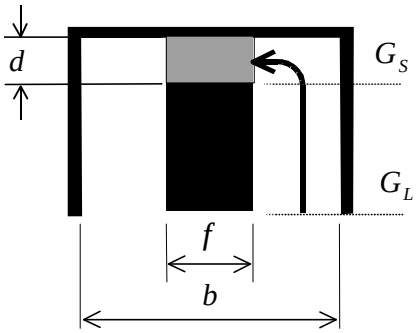

Figure 1 – Diagram of the wave propagation in a thin parallel plate capacitor terminating a coaxial waveguide.

scattering coefficient S_{11} resulting from the combination of the multiple reflection and transmission components can be expressed by equation (1):

$$S_{11} = \frac{r + e^{-gf}}{1 - re^{-gf}} \quad (1)$$, where ρ is the complex reflection coefficient for non-magnetic media; $r = \frac{1-\sqrt{e^*}}{1+\sqrt{e^*}}$, γ is the propagation constant; $g = \frac{jw}{c}\sqrt{e^*}$, e^* is the relative complex permittivity of the dielectric, $e^* = e' - je''$, w is an angular frequency and c is the speed of light in air.

On the other hand, the input admittance of the sample section Y_{in} can be expressed as a function of the S_{11} coefficient by:

$$Y_{in} = G_s \frac{1 - S_{11}}{1 + S_{11}} \quad (2)$$

where G_s is the characteristic conductance of the sample section. Combining (1) and (2) gives:

$$Y_{in} = G_s \frac{(1-r)(1-e^{-gf})}{(1+r)(1+e^{-gf})} = G_s\sqrt{e^*}\tanh(gf/2) \qquad (3)$$

Introducing $x = \frac{wf}{2c}\sqrt{e^*}$, and using a relation $\tanh(jx) = j/\cot(x)$, the equation (3) can be rewritten as:

$$Y_{in} = G_s \frac{jwf}{2c} e^* \frac{1}{x\cot x} \quad (4)$$

Equation (4) describes the input admittance of a distributed network that comprises the thin parallel-plate capacitor, filled with a dielectric of complex permittivity e^*. Using the complex capacitance notation for the sample section C^*, equation (4) may be expressed as:

$$Y_{in} = jw\, C^* \frac{1}{x\cot x} \qquad (5)$$

where $C^* = G_s \frac{f}{2c} e^*$.

In equations (4) and (5) the sample section is represented as a transmission line having electrical length of ϕ/2, where the total geometric capacitance of the sample section is obtained from the characteristic conductance per unit length.

The term $1/x\cot x$ accounts for the propagation in the sample section. If the electrical length is small in comparison to the wavelength, ϕ << λ, $x << 1$, the value of the $1/x\cot x$ approaches unity and then equation (5) simplifies to the conventional formula for the input admittance of a lumped shunt capacitance terminating a transmission line [6].

Expression for complex permittivity in frequency domain

In the actual experimental arrangement the scattering coefficient S_{11}^m is measured for a network consisting of the coaxial waveguide connected to the sample section (Fig. 1). The reference plane is set at the interface between the end of the coaxial waveguide with the characteristic conductance G_l and the dielectric sample section with the characteristic conductance G_s. The input admittance is given by:

$$Y_{in} = G_l \frac{1 - S_{11}^m}{1 + S_{11}^m} \quad (6)$$

Combining equations (4) and (6), we obtain expression (7) for complex permittivity e^* in terms of measurable quantities S_{11}^m, G_l and G_s,

$$e^* = \frac{2c}{iwgf}\frac{1 - S_{11}^m}{1 + S_{11}^m} \cdot x\cot x \qquad (7)$$

where gf is the effective line length of the sample section in reference to the coaxial line with the characteristic conductance G_l. The parameter $g = G_l/G_s$ represents a cell constant, which for a given sample geometry can be determined from measurements of materials with known permittivity. In cases where the geometry of known and unknown samples differs, the equivalent cell constant parameter can be determined by evaluating the fringing field capacitance.

Following the discussion in references [7] and [8], the complex capacitance of the specimen section consisting of parallel-plate capacitance filled with a dielectric film

of permittivity *e** and the fringing field capacitance can be calculated as follows:

$$C^* = C_p e^* + C_f = \frac{p f^2}{4d} e_0 e^* + 2 a e_0 \ln\left(\frac{b-f}{2d}\right) \quad (8)$$

where C_p is the geometric capacitance of the empty parallel-plate section, C_f represents the fringing field capacitance, f and b are the diameters of the center and outer conductor respectively as shown in Fig. 1, d is the sample thickness and e_0 is the permittivity of air. Here, $d << b - f$ and $l >> 2\pi d$, where l is the wavelength in the fringing field area. Combining (6) and (7) with (8) we obtain equation (9) that is applicable to solid film dielectrics.

$$e^* = \frac{G_l}{jwC_p}\frac{1-S_{11}^m}{1+S_{11}^m}\cdot x\cot x - \frac{C_f}{C_p} \quad (9)$$

The value of the C_f / C_p ratio depends on configuration of the sample section and decreases to zero with decreasing film thickness.

Equation (9) is an entangled expression containing complex permittivity e^* on both sides. Therefore, an iterative algorithm is required to find the value of e^* satisfying the equation for each measured value of S_{11}^m. At sufficiently low frequencies, the term $x\cot x$ approaches unity with $x \approx 0$, and equation (9) simplifies to expression (10),

$$e^* = \frac{G_l}{jwC_p}\frac{1-S_{11}^m}{1+S_{11}^m} - \frac{C_f}{C_p} \quad (10)$$

which is the conventional lumped capacitance model that can be used for initial guessing of the complex permittivity values at low frequencies.

Expression for complex permittivity in time domain

In time domain the input admittance can be expressed by using measurable TDR waves:

$$Y_{in} = G_l \frac{V_i(jw) - V_r(jw)}{V_i(jw) + V_r(jw)} \quad (11)$$

where $V_i(jw)$ and $V_r(jw)$ are the Laplace transforms of the incident and the reflected voltage waves, and G_l is the characteristic conductance of the coaxial line. By combining equations (11) and (4) we obtain expression (12) for e^* as a function of measurable incident and reflected voltage step waves, V_i and V_r respectively:

$$e^* = \frac{G_l}{jw\,C_p}\frac{V_i(jw) - V_r(jw)}{V_i(jw) + V_r(jw)}\cdot x\cot x - \frac{C_f}{C_p} \quad (12)$$

In practical measurements it is convenient to avoid using the input step wave V_i in (12), which introduces some, difficult to account for numerical errors due to finite rise time and limited flatness of the generated step voltage. Instead, reflection measurements on a standard specimen with known permittivity, such as air-gap can be utilized. The detailed measurement procedure and error analysis is given in Ref. (4).

EXPERIMENTAL

Test fixture

The broadband measurements were conducted using an experimental coaxial test fixture constructed from two APC-7 to APC 3.5 microwave adapters. The center conductor was replaced with a fixed 3.0 mm diameter pin, machined precisely to achieve flat and parallel contact between the film specimen and the 7 mm short termination. All surfaces were gold-finished. The fixture connects to the microwave instrumentation through the APC 3.5 port. In comparison to other testing configurations that utilize SMA connectors or coupling probes, this test fixture minimize coupling errors, errors caused by inductive components and radiation losses, as well as those due to change in electrical conditions established during calibration.

Materials

High dielectric constant EDC films BC2000™ and EmCap™ (PolyClad), CPly™ (3M) and HiK™ Polyimide(Dupont) were obtained from the NCMS Embedded Capacitance Project [2]. The films were formulated as composites of a polymer resin filled with ferroelectric ceramic powders and coated with copper on both sides. The 3 mm diameter circular film specimens were defined using photolithography. The dielectric permittivity of the EDC films measured by using the microstrip resonator technique at discrete frequencies is given in Tab. 1. Poly(trimethylopropane triacrylate) filled with Barium Titanate powder with an average particle size of 1 μ was formulated into 100 μm thick films [10] and used as model of the EDC dielectric

Tab. 1. Dielectric properties, ε' and tan (δ), of the EDC films of thickness *d*, measured at frequency *f*.

Material	*d* (μm)	*f* (GHz)	*e'*	*tan (d)*
BC2000™	50	0.928	3.88	0.021
EmCap™	100	0.842	38.4	0.013
CPly™	8	1.012	22.1	0.08
HiK™	48	1.093	11.8	0.01

Measurements

Dielectric measurements in frequency domain were curried out in the frequency range between 100 MHz and 10 GHz using a network analyzer (HP 8720D). One-port S_{11} (open, short and broadband load) calibration was performed using a HP 85050B APC-7 calibration kit. The reference plane established during calibration was transformed to the corresponding metal-dielectric interface by introducing an electrical delay. The specimen geometry was measured using a Mitutoyo micrometer model 293-301 with an uncertainty of ± 1 μm. The relative uncertainty in geometrical capacitance measurements was typically 2 % with the primary contribution from the uncertainty in the film thickness measurements. The relative uncertainty of S_{11} was assumed to be within the manufacturer specification for the HP 8720D. The combined relative experimental uncertainty in complex permittivity was less than 8 % while the experimental resolution of the dielectric loss tangent measurements was about 0.01. The TDR measurements were carried out using a Tektronix 11802 Digital Sampling Oscilloscope equipped with a TEK SD-24 TDR/Sampling Head. A VEE 5.0 software platform from Hewlett Packard was used for acquisition and processing of the data. Waveforms were captured in a 10 ns window typically containing 1024 data points with a resolution of 2.5 ps. The combined uncertainty in the dielectric constant obtained in time domain was evaluated using the relaxation charging time [4]. All the measurements were performed at room temperature (22 °C).

RESULTS AND DISCUSSION

Example measurements of the frequency dependent dielectric constant, ε', and the dielectric loss ε" obtained for the EDC films are plotted Fig. 2 and 3. The results obtained from the lumped capacitor model without propagation (equation 10) are also plotted for comparison.

The permittivity results obtained for the BC2000™ and EmCap™ films (Fig. 3) agree closely with the microstrip resonance results (Tab.1) where the differences are within 1 % for ε' and 4% for ε". The new propagation model gives appropriate behavior of complex permittivity of EDC films throughout the entire frequency range from 100MHz and 10GHz. The dielectric constant of BC2000™ is about 4.0 at 500 MHz and it decreases to about 3.8 at 5 GHz, which is a typical dispersion behavior observed for epoxy resins. The dielectric loss data shown in Fig. 2b are in the range of about 0.08 and are also consistent with the dielectric properties of FR−4 epoxy based laminates. The dielectric permittivity of the EmCap™ films shown in Fig. 2 is approximately 10 times larger than that of BC2000™ ,

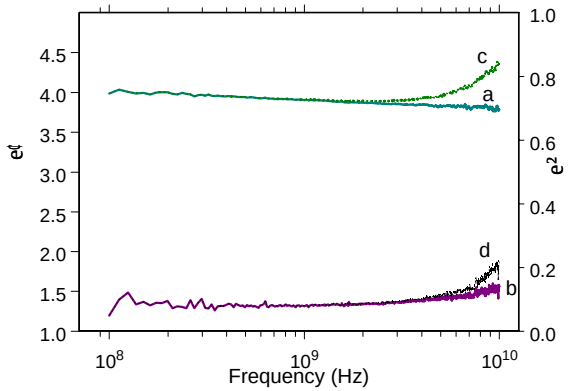

Figure 2 – Dielectric permittivity of BC2000™;
a – dielectric constant, b- dielectric loss,
c and d – dielectric constant and dielectric loss using the lumped capacitance method.

which results from the high content of ferroelectric ceramic.

The ε' of EmCap™ decreases from about 40 at 100 MHz to about 38 at 5 GHz while the dielectric loss (Fig. 2b) increases slightly from 0.15 to 0.20 with increasing frequency, which agrees with the microstrip resonance data. Results shown in Fig. 2 and 3 indicate that the new model, in which the film specimen is treated as a

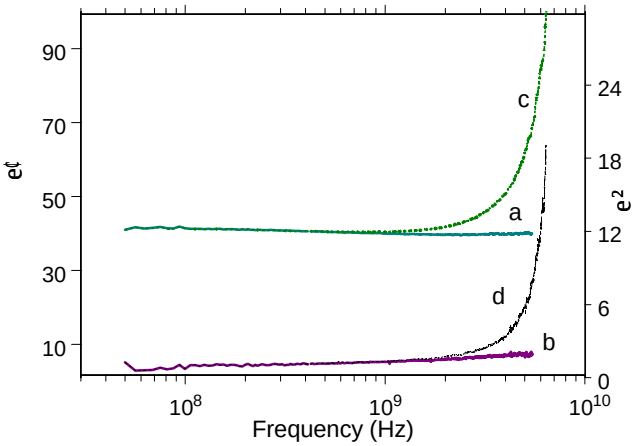

Figure 3 – Dielectric permittivity of EmCap™;
a – dielectric constant, b- dielectric loss,
c and d – dielectric constant and dielectric loss using the lumped capacitance method.

distributed component with capacitance, describes correctly the complex permittivity of low and high dielectric constant films over a broad frequency range. In contrast, the lumped capacitor model shows anomalies at frequencies above 1 GHz - 3GHz (see Fig. 2c, 2d and 3c, 3d). The value of the real part of permittivity, ε', and

the imaginary part, ε", determined from equation (10) increase as frequency increases, leading to systematic errors that at higher frequencies exceed considerably the combined experimental uncertainty. The systematic errors become larger as the dielectric constant of the film specimen increases.

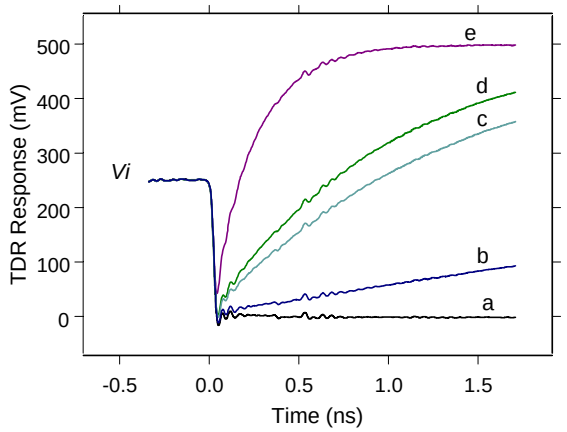

Figure 4 – TDR response from EDC films:
a) short termination, b) CPly™ c) EmCap™ , d) HiK™ e) BC2000™

Fig. 4 shows the TDR response produced by a 250 mV step V_i reflected at EDC films terminating the coaxial test fixture (Fig. 1).
When the incident step is reflected at an open circuit (C ≈ 0, Z ≈ ∞), both the incident wave and the reflected wave are in phase, $V_r = V_i$, and combine after the delay time t_0 , (here t_0 is set to zero) resulting in the reflected amplitude of $2V_i$. In comparison, the wave reflected at a zero impedance circuit (Z = 0 Ω) is out of phase by 180° in respect to the incident wave, $V_r = - V_i$, and thus the initial step returns to zero after the transition time t_0 , as it is illustrated in Figure 4a. For EDC films, the resulting reflection exhibits a positive going transfer that is exponential in time. The shape of the reflected wave V_r depends on the nature and magnitude of mismatch between the coaxial line impedance Z_l (here Z_l = 50 Ω) and impedance of the termination. Having determined the dielectric permittivity in frequency domain, the complex impedance of the EDC can be expressed as follows:

$$Z_{in} = \frac{1}{jw\, C_p e^* - j/w\, L}$$

It is seen in Fig. 4 that at time zero (or at highest frequencies ω) all the EDC specimens appear as a short circuit indicating a pure capacitive behavior. At longer times, the voltage builds up across the complex capacitance C_p e^* increasing its impedance until it effectively becomes an open circuit. The inductive circuit components j/wL , which are a common source of error in impedance measurements, do not contribute to the measured response and therefore, in this the test fixture configuration, can be neglected.

The TDR response measured by the new test technique can be used directly to determine the efficiency of the EDC materials. The results can be transformed into impedance reading by putting in expression (6) or (10) $S_{11}^m = V_r / V_i$ and $Z_{in} = 1/Y_{in}$.
The best performance is indicated by the response close to that of zero impedance (short) termination, as it is shown in Fig. 4b for CPly™. The thickness of the CPly™ films was only about 8 μm. Therefore in comparison to other EDC materials tested, the CPly™ had the highest geometric capacitance C_p that compensated its somewhat lower dielectric constant than that of EmCap™ (Tab. 1). For the same geometric capacitance lower impedance will result from a dielectric material with higher complex permittivity e^*.

In order to provide adequate amount of charge without excessive change in the VDD level the EDC impedance should be low ($Z_{EDC} \approx 0$) in a broad range of frequencies. In Fig 4, the standard 3 mm diameter capacitor can source the charge as long as the amplitude of the response is lower than the amplitude of the input step V_i. Decreasing the dielectric thickness between the planes and increasing the dielectric constant of the inter-plane dielectric can realize this requirement.
On the other hand, at frequencies approaching 1 GHz

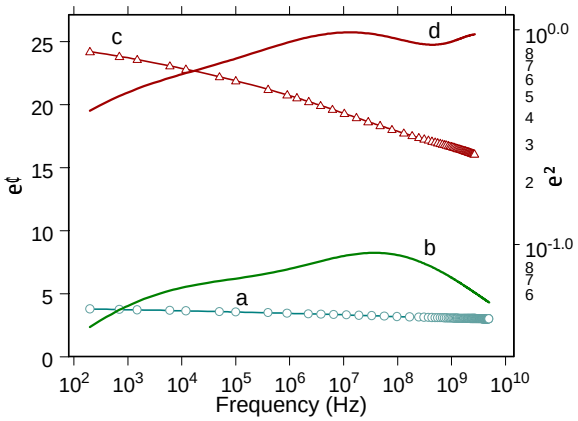

Figure 5 – Broadband dielectric permittivity of the polymer matrix (plots a - ε′ and b- ε″) and the corresponding composite loaded with 30 vol.% of ferrolectric powder (plots c - ε′ and d- ε″).

and above the EDC plane in a circuit board is no longer electrically small and typically exhibits undesired rapid oscillation of impedance at resonant frequencies. The resonant behavior can be suppressed by introducing a

loss mechanism into EDC as a frequency tailored dielectric loss or/and conductor loss. Both factors independently contribute to lowering the broadband impedance.

The EDC materials measured in a functional test vehicle configuration showed supprisingly flat impedance characteristic [1], indicating a much lower Q factor than it could be expected from the dielectric properties of the organic and ceramic constituents. Our study provides clear evidence that the binary mixtures of organic polymer resins with ferroelectric powder indeed exhibit an intrinsic high frequency loss.
Figure 5 shows broadband permittivity of the model polymer resin and that of the corresponding high dielectric constant composite. It is seen that in comparison to the polymer matrix, the composite material exhibits a magnified loss with peak value at frequency of about 20 MHz. We found that the position of the loss peak is determined by the dielectric relaxation of the polymer backbone while its magnitude depends on the dielectric dispersion, and therefore, is amplified by the content and permittivity of the ferroelectric component. A polymer matrix with shorter relaxation time will likely shift the loss peak position to higher frequencies, while higher polarizability can increase the loss magnitude. Thus, both the value of the dielectric constant as well as the position and magnitude of the loss peak can be controlled by modifying the composition of the dielectric material. In most polymers, molecular relaxations cease at frequencies above a few gigahertzes. To suppress the resonant behavior at these higher frequencies, a conductor loss may be by introduced in form of a semi-conducting layer at the metal dielectric interface. For example, a layer of copper oxide, which is a typical surface modifier to promote adhesion between copper conductor and polymer resin in copper-cladded epoxy laminates, can be used to attenuate higher-order resonant modes.

SUMMARY

We evaluated the impedance and dielectric permittivity characteristics of embedded decoupling capacitance films in time domain and at frequencies of 50 MHz to 10 GHz. The film specimen is treated as a network consisting of a transmission line with capacitance terminating coaxial air-line, for which we developed a suitable propagation model. This allowed us to overcome the limitations of existing lumped element methods and extend the measurements to frequencies of practical importance, above 1 GHz. It was found that polymer composites films filled with ferroelectric ceramic could provide low impedance not only through a high capacitance, but also due to intrinsic high frequency loss. At frequencies above polymer molecular relaxations, conductor losses may be introduced to attenuate the higher-order resonant modes. This makes polymer composite films very efficient as a broadband embedded decoupling capacitance that can secure the signal integrity and minimize the EMI noise in high-speed circuits operating at microwave frequencies.

REFERENCES

1. T. Hubbing and M.Xu, “Electronic design considerations for printed circuit boards with embedded capacitance”, Proceedings of the NCMS Conference on Embedded Capacitance, February 28-29, 2000, Tempe AZ.
2. P. Lee and R. Chabornneau (Ed.), Embedded Capacitance Project Report, NCMS, 3025 Boardwalk, Ann Arbor, MI 48108, August, 2000.
3. F. I. Mopsik, “Extended frequency range dielectric measurements of thin films”, Rev. Sci. Instr. vol.71, pp2456-2460, 2000.
4. J. Obrzut and R. Nozaki, “Permittivity measurements of high dielectric constant films at microwave frequencies”, Proceeding of the IPC Printed Circuits Expo 2000, April 1-5, San Diego, CA, section. S8-6.
5. R. Nozaki and J. Obrzut, “Broadband complex permittivity measurements of solid films at microwave frequencies”, submitted to IEEE Trans. Microwave Measurements and Instrumentation
6. M. A. Stuchly and S. S. Stuchly, “Coaxial line reflection methods for measuring dielectric properties of biological substances at radio and microwave frequencies: A review”, IEEE Trans. Instrum. Meas., vol. 29, pp 176-183, 1980.
7. N. Marcuvitz, Waveguide Handbook. McGraw-Hill, New York: 1951.
8. M. F. Iskander and S. S. Stuchly, “Fringing field effect in the lumped-capacitance method for permittivity measurements”, IEEE Trans. Instrum. Meas., vol. IM-27, pp. 107-109, 1978.
9. J. Obrzut, “Evaluation of dielectric properties of polymer thin-film materials for application in embedded capacitance”, Proceedings of the NCMS Conference on Embedded Capacitance, February 28-29, 2000, Tempe AZ.
10. C. K. Chiang, R. Popielarz, R. Nozaki and J. Obrzut, Mat. Res. Soc. Symp. Proc., vol. 628 pp. CC6.13. (2000).

ACKNOWLEDGMENTS

This work was supported in part by the NIST Advanced Technology Program and through the NIST MSEL Director’s Research Fund.

DISCLAIMER

Certain materials and equipment identified in this manuscript are solely for specifying the experimental procedures and do not imply endorsement by NIST or that they are necessary the best for these purposes.